SciPost Physics Proceedings Submission

Recent Results from the Long-Baseline (LBL) Neutrino Oscillation Experiments

P. Fernández

IFIC (CSIC & University of Valencia), Valencia, Spain
* *pablo.fer@cern.ch*

October 31, 2018

Proceedings for the 15th International Workshop on Tau Lepton Physics, Amsterdam, The Netherlands, 24-28 September 2018
scipost.org/SciPostPhysProc.Tau2018

Abstract

The results from the current long-baseline neutrino oscillation experiments are reviewed. These experiments are designed to measure the remaining unknown neutrino oscillation parameters via the oscillation of accelerator neutrinos over long distances.
The performance of these experiments and their results are reviewed and discussed, giving a precise picture of the current status of the measurements for the neutrino mass ordering, the value of Δm^2_{32}, the θ_{23} and the lepton CP-violating phase, δ_{CP}.

Contents

1 Introduction

Long-baseline neutrino oscillation experiments have provided a great progress in our knowledge of the neutrino properties as compared to the experiments measuring neutrinos from natural sources. Thanks to its efficient design and operation, they have been able to get us closer to the measurement of the most challenging neutrino oscillation parameters, those are the θ_{23} mixing angle, the neutrino mass ordering and the CP-violating phase of the lepton sector.
In this conference paper the current status of the long-baseline neutrino oscillation experiments, first, in section 2, reviewing and summarizing the physics of neutrino oscillations with its main remaining unknows, and how LBL are built so they can provide the most precise measuremnts for these unknown parameters. Then in section 3, the current LBL experiments are reviwed and their results discussed to give an overall picture of the current status of neutrino oscillation physics. The T2K, NOνA and MINOS/MINOS+ experiments are described in 3.1, 3.2 and 3.4. The OPERA experiment was covered by a dedicated talk in this same conference, so it is not mentioned here.
Finally, the results of all these experiments are summarized in 4 and the most important points from these experiments are shown in 5.

2 Physics of Neutrino Oscillations

The first evidence of neutrino oscillations was done by the Super-Kamiokande experiment in 1998 and using atmospheric neutrinos.
The neutrino oscillations arise from the fact that neutrinos are not massless as assumed by the Standard Model (SM), making neutrino oscillations the first evidence of physics beyond the SM. The SM predicts the existence of three neutrinos and this is the framework assumed for the rest of this paper.
Neutrinos do not share the same flavor (interaction) and mass (propagation) eigenstates and they are tranformed by a non-diagonal unitary matrix with four degrees of freedom, parametrized by three mixing angles θ_{12}, θ_{13} and θ_{23} and a CP-violating phase, δ_{CP}. This is the PMNS matrix,

$$\begin{pmatrix}\nu_e\\ \nu_\mu\\ \nu_\tau\end{pmatrix} = U_{PMNS}\begin{pmatrix}\nu_1\\ \nu_2\\ \nu_3\end{pmatrix} \tag{1}$$

$$U_{PMNS} = \begin{pmatrix}1 & 0 & 0\\ 0 & c_{23} & s_{23}\\ 0 & -s_{23} & c_{23}\end{pmatrix}\begin{pmatrix}c_{13} & 0 & s_{13}e^{-i\delta_{CP}}\\ 0 & 1 & 0\\ -s_{13}e^{i\delta_{CP}} & 0 & c_{13}\end{pmatrix}\begin{pmatrix}c_{12} & s_{12} & 0\\ -s_{12} & c_{12} & 0\\ 0 & 0 & 1\end{pmatrix} \tag{2}$$

where $c_{ij} = \cos\theta_{ij}$ and $s_{ij} = \sin\theta_{ij}$.
This means that after neutrinos have propagated freely through space they can be detected with a flavour different from that of their origin. This phenomenon is called neutrino oscillations and the probability of a neutrino to change its flavour after a free propagation in vaccum is given by the following expression:

$$P_{\nu_l\to\nu_{l'}}(L/e) \approx \sum_{ij} U^{l',i}_{PMNS}(U^{l,i}_{PMNS})^*(U^{l',j}_{PMNS})^*U^{l,j}_{PMNS}e^{-i\frac{\Delta m^2_{ij}}{2}\frac{L}{E}} \tag{3}$$

These means that the neutrino oscillation probabilities depend on the four parameters of the PMNS matrix, the ratio between the distance travelled by the neutrinos and their energy and also on two independent mass square differences, In the three flavor neutrino framework, there are six independent oscillation parameters, the three mixing angles and the δ_{CP} phase from the PMNS matrix and the two neutrino square mass diferences.

$$\Delta m^2_{21} = m^2_2 - m^2_1,\ \Delta m^2_{31} = m^2_3 - m^2_1 \tag{4}$$

The third mass square difference is just a linear combination of the other two $\Delta m^2_{32} = \Delta m^2_{31} - \Delta m^2_{21}$.

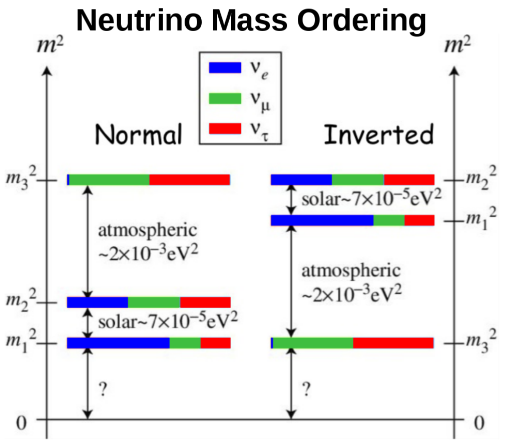

Figure 1: Two possible neutrino mass orderings allowed.

This definition means that there are two possibilities for the ordering of the neutrino masses, normal (neutrino third mass eigenstate is the heaviest) and inverted (neutrino third mass eigenstate is the lightest), as shown in 1.

As LBL mainly produce muon (anti)neutrinos to be propagated to the detector, there are basically two oscillation channels that matters for measuring the oscillation parameters. The disappearance channel is the survival probability of the produced muon (anti)neutrinos at the accelerator facility. This channel is most sensitive to the θ_{23} and the neutrino mass ordering.

$$P(\overset{(-)}{\nu}_\mu \rightarrow \overset{(-)}{\nu}_\mu) \cong 1 - 4\sin^2\theta_{23}\cos^2\theta^M_{13}(1 - \sin^2\theta^2_{23}\cos^2\theta^M_{13})\sin^2\left(\tilde{\Delta}\frac{L}{E}\right) \tag{5}$$

where,

$$\begin{gathered}\tilde{\Delta} = \frac{\Delta m^2_{32} + \Delta m^2_{21}\sin^2\theta_{12} + \Delta m^2_{21}\cos\delta_{CP}\sin 2\theta_{12}\sin\theta_{13}\tan\theta_{23}}{4} \\ \sin^2\theta^M_{13} = \frac{\sin^2 2\theta_{13}}{\sin^2 2\theta_{13} + (A - \cos 2\theta_{13})^2},\ A = \sqrt{2}G_F N^{man}_e \frac{2E}{\Delta m^2_{31}}\end{gathered} \tag{6}$$

The apearance channel, on the other hand, is the probability of the muon (anti)neutrinos to turn into electron (anti)neutrinos and is most sensitive to the θ_{13} mixing angle, which dominates the expression, the neutrino mass hierarchy and to the CP-violating phase, δ_{CP}.

$$\begin{aligned}P(\overset{(-)}{\nu}_\mu \rightarrow \overset{(-)}{\nu}_e) \cong & \underbrace{\sin^2\theta_{23}\frac{\sin^2 2\theta_{13}}{(A-1)^2}\sin^2\left((A-1)\Delta\frac{L}{E}\right)}_{\text{leading term, }\theta_{13}} + \alpha^2\cos^2\theta_{23}\frac{\sin^2 2\theta_{12}}{A^2}\sin^2\left(A\Delta\frac{L}{E}\right) \\ & + \frac{\alpha J_{CP}}{A(1-A)}\sin\left(A\Delta\frac{L}{E}\right)\sin\left(\Delta(1-A)\frac{L}{E}\right)\left(\underbrace{\cot\delta_{CP}\cos\left(\Delta\frac{L}{E}\right)}_{\text{CP conserving term}} \underbrace{\pm\sin\left(\Delta\frac{L}{E}\right)}_{\text{CP violating term}}\right)\end{aligned} \tag{7}$$

where,

$$\alpha = \frac{\Delta m^2_{21}}{\Delta m^2_{31}},\ \Delta = \frac{\Delta m^2_{31}}{4},\ J_{CP} = \cos\theta_{13}\sin 2\theta_{12}\sin 2\theta_{23}\sin 2\theta_{13}\sin\delta_{CP} \tag{8}$$

These expressions differ slighly from those obtained from 3 beacuse they also contain variations due to the matter effects of the Earth during the propagation of neutrinos.

3 LBL Neutrino Oscillation Experiments

The basic setup of current LBL neutrino experiments consist on near and far detectors to which (anti)neutrinos produced at accelerators are thrown.
Since the neutrino probabilities are modulated by L/E ratio, LBL expeiments are designed so this ratio is such that the disappearance and appearance channels are optimized.
The goal of long-baseline neutrino experiments is to measure the remaining neutrino unknown parameters, with special focus on the CP phase due to its implications, being a potential explanation for the matter-antimatter inbalance in our universe.

3.1 The T2K Experiment

The T2K experiment is located in Japan and its focus is in the measurement of the θ_{23}, θ_{13} and δ_{CP}. It uses the J-PARC neutrino facility at Tokai, which produces mainly ν_μ and $\overline{\nu}_\mu$, depending on the beam mode. These neutrinos are then detected at the ND280 near detector facility and the Super-Kamiokande far detector.

Figure 2: Geographical view of the T2K experiment layout.

The T2K beam
The J-PARC neutrino beam has been operating this year with a mean power of 485 kW, achieving maxima of more than 500 kW. The total amount of protons-on-target (POT) accumulated during the T2K operation is $3.2 \cdot 10^{21}$, $1.51 \cdot 10^{21}$ in neutrino mode and $1.65 \cdot 10^{21}$ in antineutrino mode.

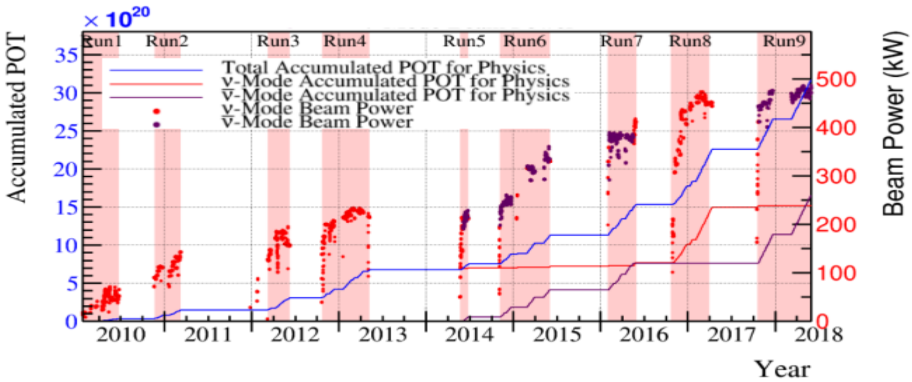

Figure 3: Accumulated POT and neutrino beam power output during the T2K operation.

The direction of the beam is not aligned with the ND280 near detector and the Super-Kamiokande far detector, but 2.5^0 off-axis. T2K was the first experiment to implement this technique due to its advantages. As shown in 4, with the 2.5^0 off-axis setup, the neutrino spectrum is narrower than for other configurations peaking at 0.7 GeV, just where the maximum of the appearance channel and the minimum of the disappearence channels are.

Due to its enormous success, it has been agreed to extend the operation of the J-PARC neutrino beam until 2026 with the aim of achieving $2 \cdot 10^{22}$ POT. This will suppose the extension of the T2K experiment, T2K phase-II.

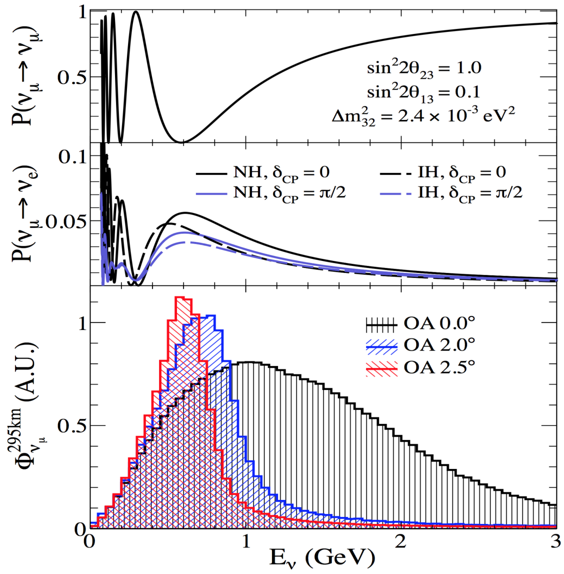

Figure 4: The plots show the T2K disappearance and appearance channel probabilities as well as the neutrino spectrum at the far detector assuming different off-axis configurations.

The T2K detectors

T2K near detector as well, which carries cross-section, energy spectrum and flux studies of the neutrino beam. This provides great knowledge about the neutrino characteristics, decreasing the associated systematic errors. ND280 is a compendium of various facilities, placed 280 m from J-PARC. It is formed by INGRID and ND280.

- ND280: This is placed 2.5^0 off-axis and composed of π^0 detector and calorimeter, an electromagnetic calorimeter, a muon detector, fine grained detectors (FGD) and argon time projection chambers (TPCs). It will be upgraded for phase-II to reduce systematics up to 4%.
- INGRID: This detector is on-axis and is a scintillation light detector made up by sixteen modules of iron plates and and eleven tracking scintillators each.

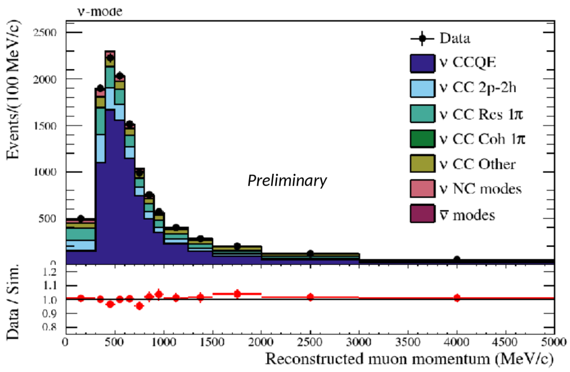

Figure 5: Two possible neutrino mass orderings allowed.

Due to the high neutrino flux at the near detector, studies concerning neutrino cross-section and reduction of the systematic errors related to the neutrino flux and interactions at the far detector.

Super-Kamiokande is the far detector, a water-Cherenkov detector with 50 kton of ultra-pure water located in the Kamioka mine under 1000 m of rock (2700 m.w.e.). It is located 295 km from the neutrino beam and optically divided into inner and outer detector.

- The inner detecor is used for physics analysis and composed by 11,143 20”-PMT facing inwards with 40% photo-coverage
- The outer detector is used as veto for cosmic rays and made up of 1,885 8”-PMT facing outwards

Super-Kamiokande is currently being upgraded and refurbished for disolving Gd into the ultra-pure water (SuperK-Gd), enhancing hugely its neutron-tagging capabilities. SuperK-Gd will operate during T2K phase-II.
In addition, the NA61/SHINE hadron production experiment at CERN provides input for reducing the T2K flux uncertainties to $\sim 5\%$.

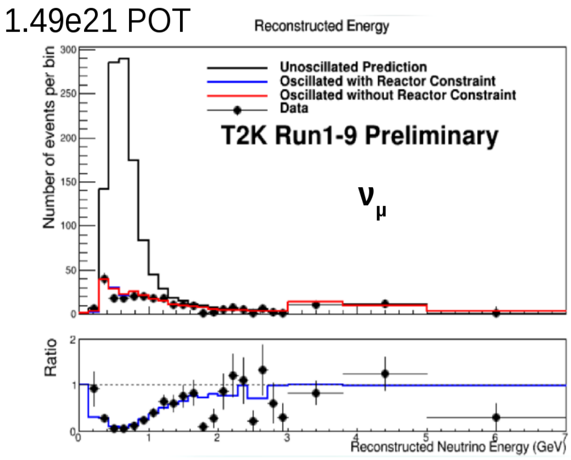

Figure 6: Two possible neutrino mass orderings allowed.

T2K neutrino oscillation results

The analysis strategy for the oscillation parameters is to compare the observed event rates at SK with the predictions under oscillation hypothesis with inputs from the near detectors. The next table shows the rate prediction for different values of δ_{CP}.

Sample	**Prediction**				**Data**
	$\delta_{CP} = -\pi/2$	$\delta_{CP} = 0$	$\delta_{CP} = \pi/2$	$\delta_{CP} = \pi$	
FHC 1R(ing) μ	268.5	268.2	268.5	268.9	243
RHC 1R(ing) μ	95.5	95.3	95.5	95.8	102
FHC 1R e 0 decay-e	73.8	61.6	50.0	62.2	75
FHC 1R e 1 decay-e	6.9	6.0	4.9	5.8	15
RHC 1R e 0 decay-e	11.8	13.4	14.9	13.2	9

Next, the results for the θ_{23} and Δm^2_{32} from T2K with reactor data constraints. These results show a preference for the θ_{23} second octant, although lower values are less than 2σ away. Since the neutrino mass ordering is yet to be determined, the fit is done for both, normal and inverted, orderings.

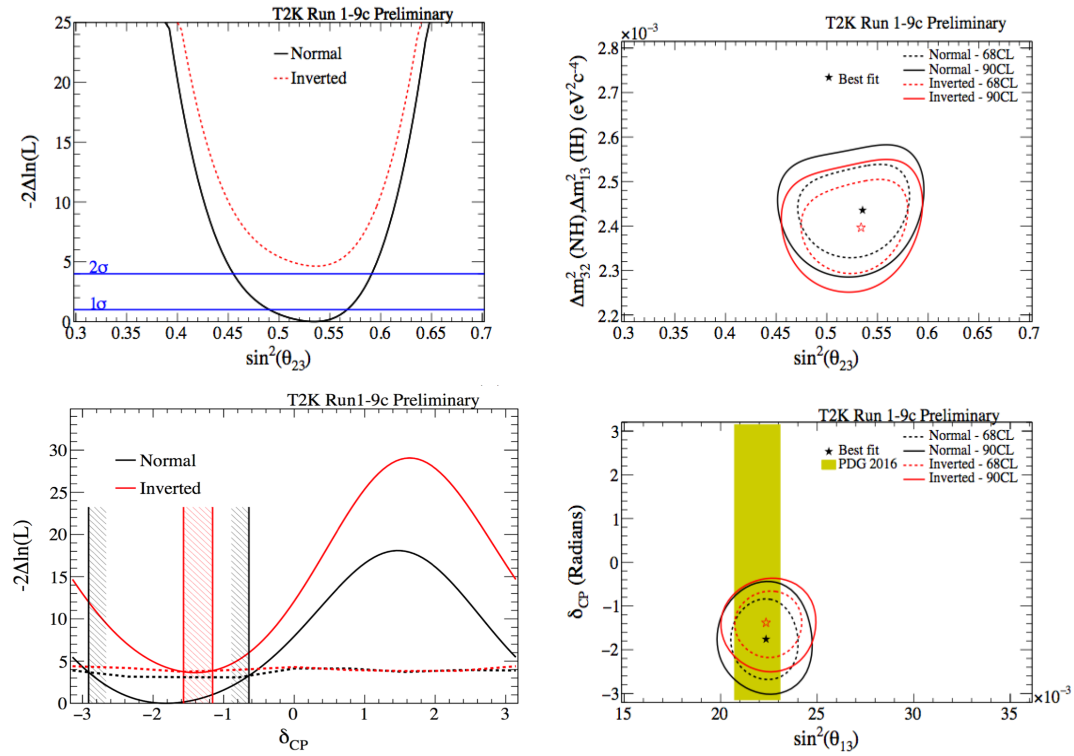

Figure 7: T2K latest results for the relevant oscillation parameters assuming the constraints given by reactor experiments and for both mass orderings. From left to right and tom top to bottom: χ^2 curve for θ_{23}, 2D contours for Δm^2_{32} and θ_{23}, χ^2 curve for δ_{CP} and 2D contours for δ_{CP} and θ_{13}.

T2K results for the Δm^2_{32} and θ_{23} assuming both neutrino mass orderings are shown in the next table.

	Normal Ordering	**Inverted Ordering**
$\sin^2\theta_{23}$	$0.536^{+0.031}_{-0.046}$	$0.536^{+0.031}_{-0.041}$
Δm^2_{32} $(10^{-3}eV^2)$	2.434 ± 0.064	$2.410^{+0.062}_{-0.063}$

The results for the δ_{CP} parameter show that the best fit is placed at large and negative values for both neutrino mass orderings, disfavoring CP-conserving values by more than the 2σ.

	Mass Ordering	δ_{CP} (rad)
Best Fit	NH (2.0σ)	-0.57π

3.2 The NOνA Experiment

The NOνA experiment is located in the US. It is also composed by near and far detectors and uses the Fermilab main injector as neutrino source.

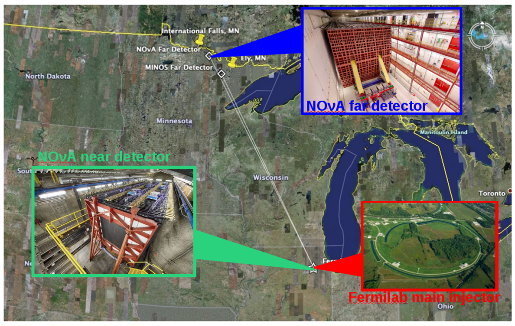

Figure 8: Geographical view of the NOνA experiment layout.

The NoνA beam

The Fermilab neutrino main injector (NuMI) produces muon neutrinos and antineutrinos and can also run in neutrino or antineutrino mode. This is the most powerful neutrino beam in the world, it has been running at the nominal 700 kW power since January 2017. Since the start of the NOνA experiment, $8.85 \cdot 10^{20}$ POT in neutrino mode and $6.91 \cdot 10^{20}$ POT in antineutrino mode have been accumulated.

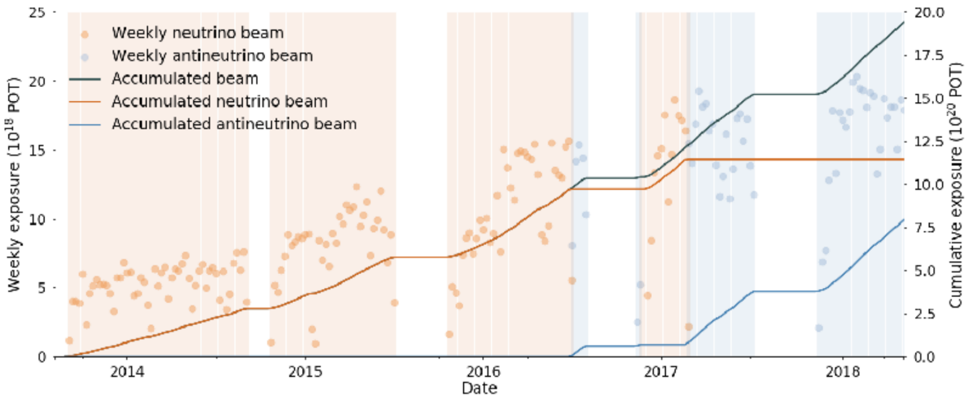

Figure 9: Accumulated POT of the NOνA experiment with time in both, neutrino and antineutrino beam modes.

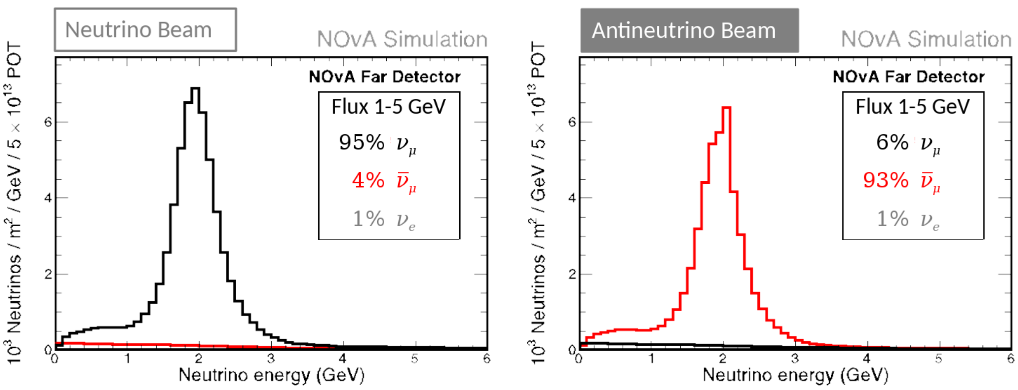

Figure 10: Neutrino spectrum simulation as seen by the NOνA far detector assuming no oscillations.

The mean neutrino energy is $\langle E_\nu \rangle \sim 1.9$ GeV and directed 14.6 mrad ($\sim 0.84^0$) off-axis with respect to the far and near detectors. As in T2K, this technique provides a narrow neutrino spectrum at the appearence maximum and disappearence minimum, optimizing the measurement of the neutrino oscillation parameters.

The NoνA detectors

The NOνA experiment is composed by two identical, except for the size, detectors and located 1 km (near detector) and 810 km (far detector) from the neutrino production point.
These detectors are tracking calorimeters made up of 344,000 cells of extruded and highly reflective plastic PVC filled with liquid scintillator. Each cell of the detectors is 3.9 cm wide, 6.0 cm deep.

- Near detector: Each cell is 3.9 m long and contains a total mass of 290 ton. To enhance muon containment, the downstream end has an additional ten layers of 10-cm-thick steel plates.
- Far detector: Each cell is 15.5 m long and it contains 14 kton.

The signal from each liquid scintillator cell is read out through a wavelength-shifting fiber (WLS). The fiber-end readout consists of a single pixel of a 32 pixel avalanche photo diode (APD) array.

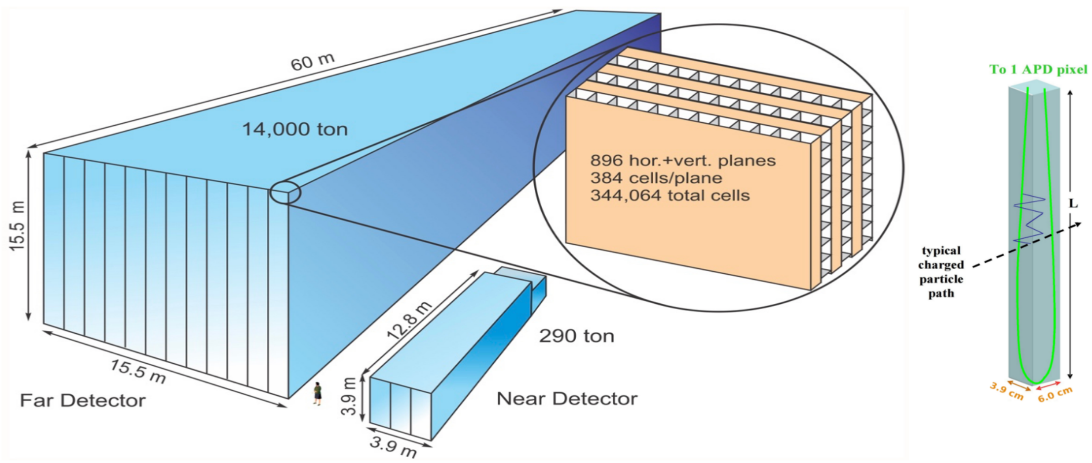

Figure 11: Schematic view of the NOνA near and far detectors with its components.

The near detector is located about 100 m underground, serving for reducing the systematic uncertainties related to the flux predictions and also conducts cross-section studies. The fact that near and far detectors share the same technology and setup is crucial for the understanding and cancelation of the systematic errors.

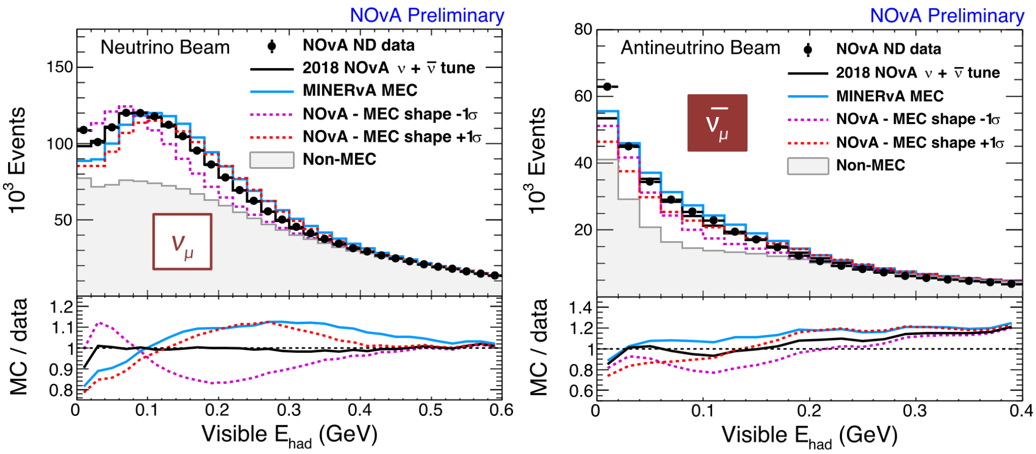

Figure 12: NOνA neutrino spectrum at the near detector for both beam configurations. The Monte Carlo simulation is tuned according to the inputs from the data in order to obtain a more accurate simulation for the far detector neutrino flux and cross-section.

The far detector is placed on the surface under a concrete and barite overburden, which stops a significant fraction of the cosmic rays.

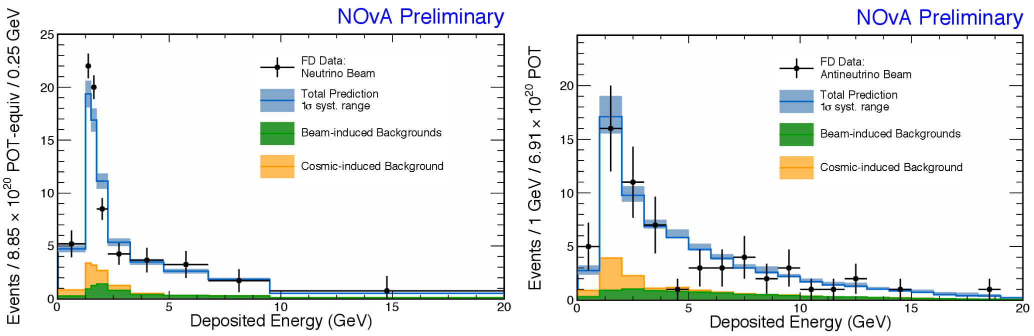

Figure 13: Simulation and data reconstructed neutrino spectrum at the far detector.

NOνA neutrino oscillation results

Despite being very different experiments, the NOνA and T2K analysis startegies are the same. The far detector event rates are compared with the oscillation predictions, and near detector data is used to reduce uncertainties related to the beam flux and the cross-section interactions. Figure 15 shows different predictions for the NOνA assuming different values of the neutrino oscillation parameters together with the actual data point in terms of the neutrino and antineutrino events rates. Data agrees with simulation showing a preference for the normal mass ordering and the second octant of θ_{23}.

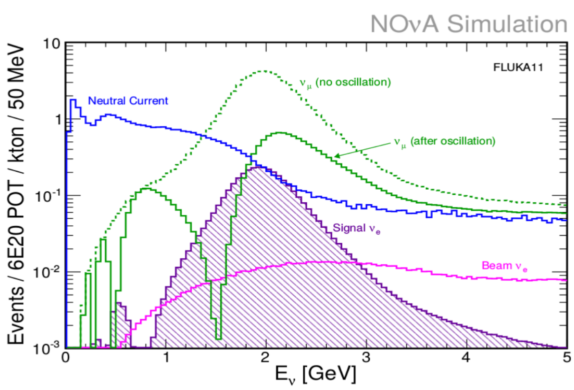

Figure 14: Simulated oscillated and unoscillated true energy neutrino spectrum of the different components of the neutrino beam.

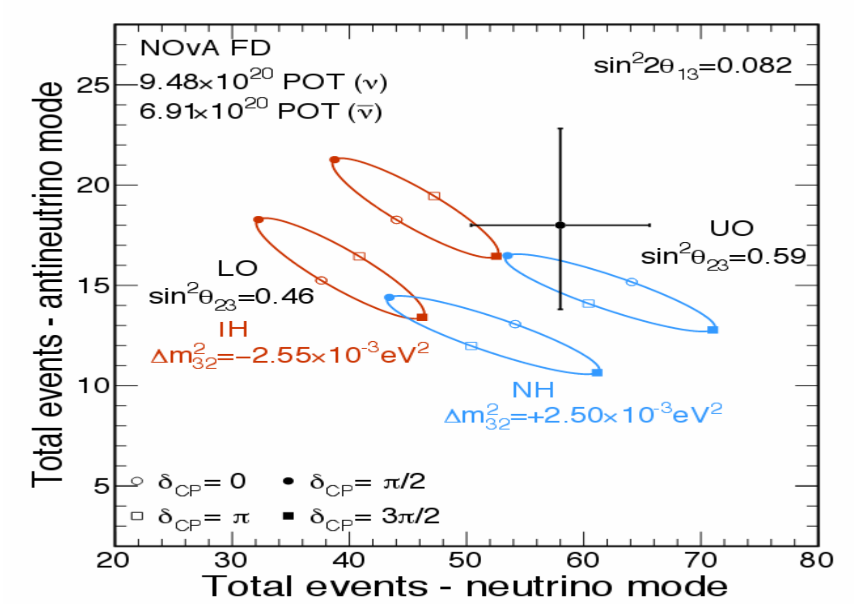

Figure 15: Comparisson of oscillated event rates between data and Monte Carlo simulation.

Next, the results of the NOνA experiment are summarize in figures 16 and 17. These results are in agreement with the previous ones from T2K, this results in more complte scenario of the remaining unkwowns of the neutrino oscillation parameters.

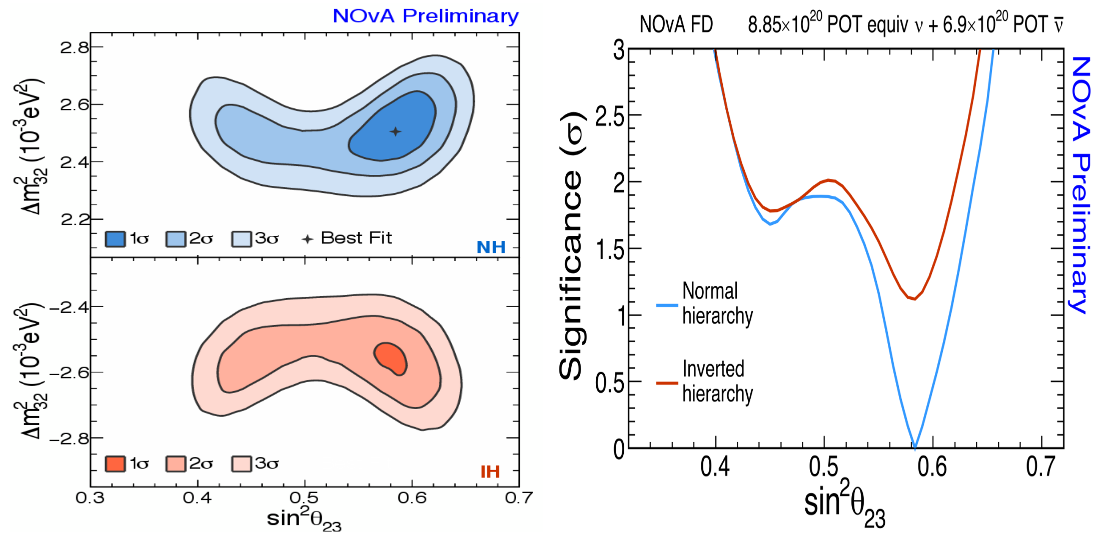

Figure 16: NOνA latest results for Δm^2_{32} and θ_{23}. Left plot shows the 2D contours for the Δm^2_{32} and θ_{23} parameters and assuming both neutrino mass orderings. Right plot shows the χ^2 curve for θ_{23}.

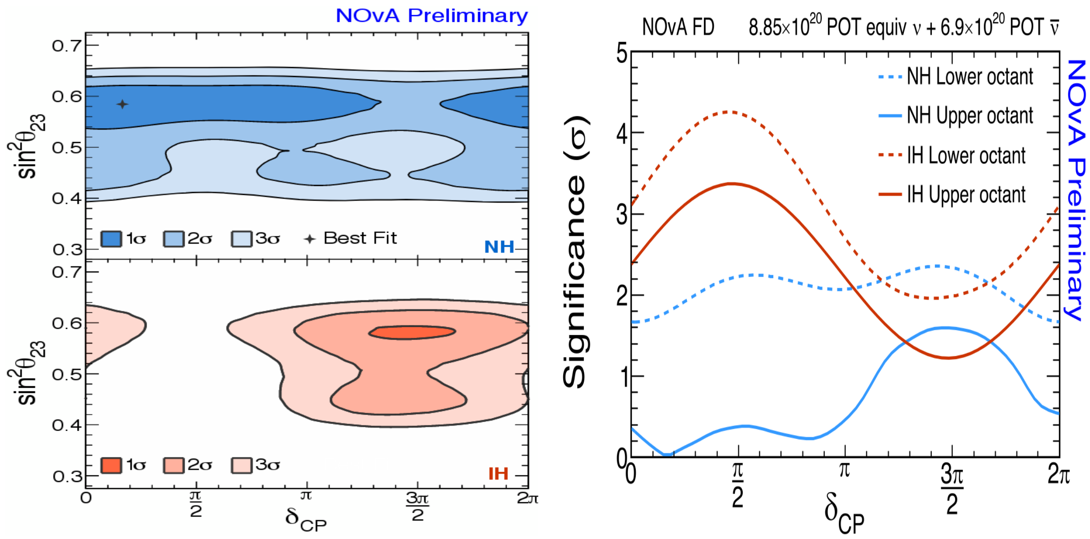

Figure 17: NOνA latest results for θ_{23} and δ_{CP}. Left plot shows the 2D contours for the θ_{23} and the δ_{CP} parameters and assuming both neutrino mass orderings. Right plot shows the χ^2 curve for δ_{CP}.

The normal mass ordering and the second octant of θ_{23} are preferred, and there is also a slight preference for large and negative values of δ_{CP}. Next table shows the best fit values given by the current NOνA data.

	Mass Ordering	$\sin^2\theta_{23}$	Δm^2_{32} (10^{-3} eV^2)	δ_{CP}
Best Fit	NH (1.8σ)	0.58 ± 0.03	$2.51^{+0.12}_{-0.08}$	-0.83π

3.3 T2K and NOνA Joint Neutrino Oscillation Analysis

Given the huge success of the T2K and NOνA experiments, it has been agreed, by the two collaborations, the formation of a working group to perform a combined analysis of their data in order to enhance the measurements of neutrino oscillation parameters made by each experiment individually. This joint analysis is forseen for 2021.

3.4 The MINOS/MINOS+ Experiment

MINOS was mainly dedicated to measure the atmospheric oscillation parameters and MINOS+ is more focused on the additional sterile neutrinos search.

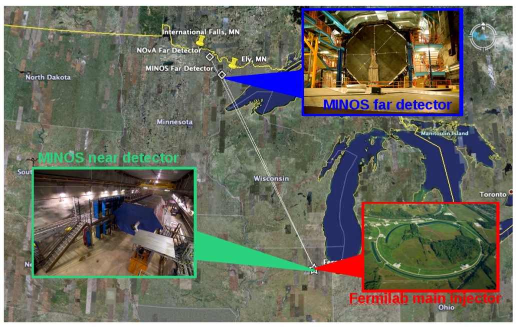

Figure 18: Geographical view of the MINOS/MINOS+ experiment layout.

The MINOS and MINOS+ beam

They use the NuMI beam, the same as the NOνA experiment:

- MINOS period: The neutrino mean energy is $\sim$ 3 GeV and has accumulated during its operation $10.56 \cdot 10^{20}$ POT in ν-mode and $3.36 \cdot 10^{20}$ POT in $\overline{\nu}$-mode.
- MINOS+ period: The neutrino mean energy is $\sim$ 7 GeV and, so far, has accumulated $9.69 \cdot 10^{20}$ POT in ν-mode.

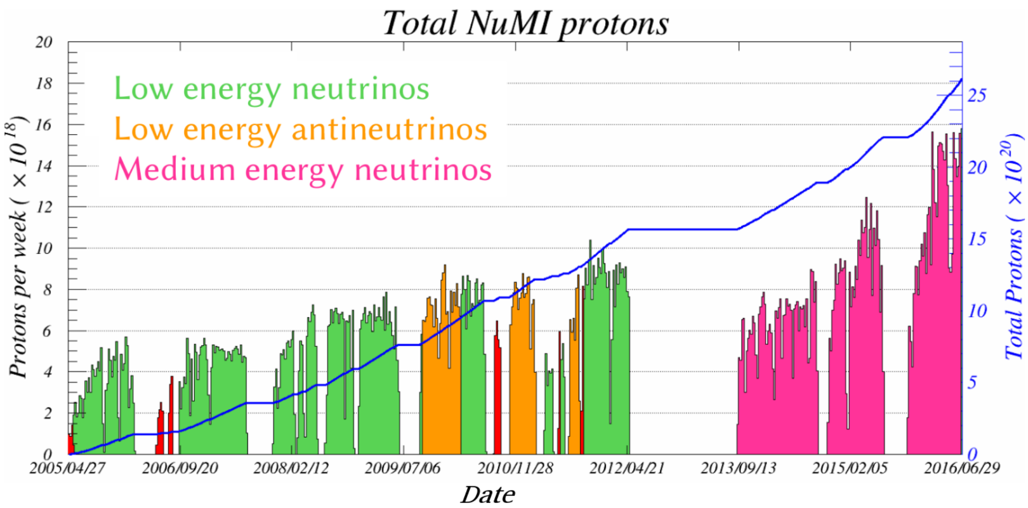

Figure 19: Accumulation of POT by the MINOS and MINOS+ experiments during their operation.

The MINOS and MINOS+ detectors

As happens for the NOνA detector, both, near and far, detectors share the same technology, but in his case they are aligned with the beam axis, do not use the previously explained off-axis layout.
The two MINOS detectors are iron-scintillator tracking calorimeters which consist of planes of steel and planes of 1 cm thick plastic scintillator. Both detectors are magnetised with a ∼1.3 T magnetic field, allowing the identification of the charged particles and improving their energy reconstruction.

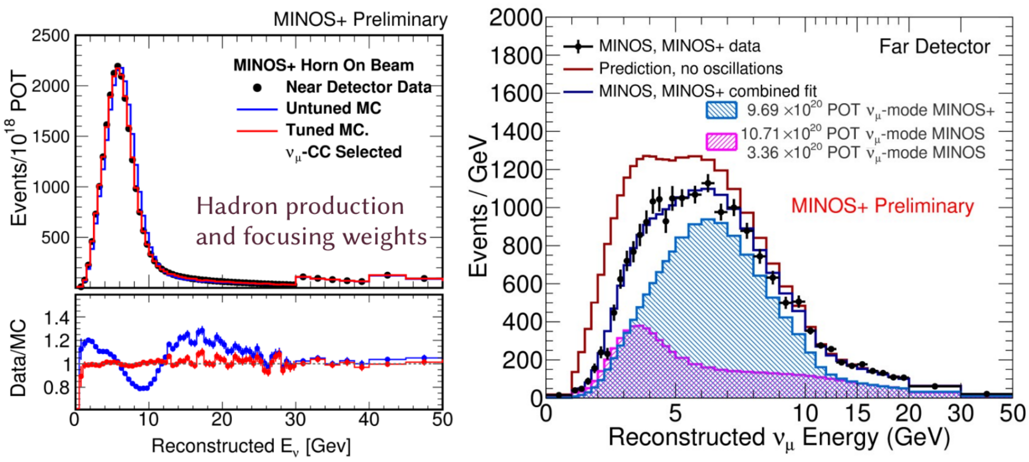

Figure 20: Comparisson plots of the reconstructed neutrino spectrum at near and far detectors.

- Near Detector: It is located 1 km from the neutrino target and 100 m underground, containing 1 kton of mass.

- Far Detector: Located 735 km from the neutrino target in the Soudan mine, 716 m underground and has 5.4 kton mass.

As in the previous experiments, the near detector has a crucial role in reducing the systematic uncertainties at the far detector, particularly in this case, where both detectors share the same techonology.

MINOS and MINOS+ neutrino oscillation results

The analysis strategy of MINOS and MINOS+ for the measurement neutrino oscillation parameters is similar to T2K and NOνA experiments.
Figure 21 shows the current results from the combined analysis of MINOS and MINOS+.

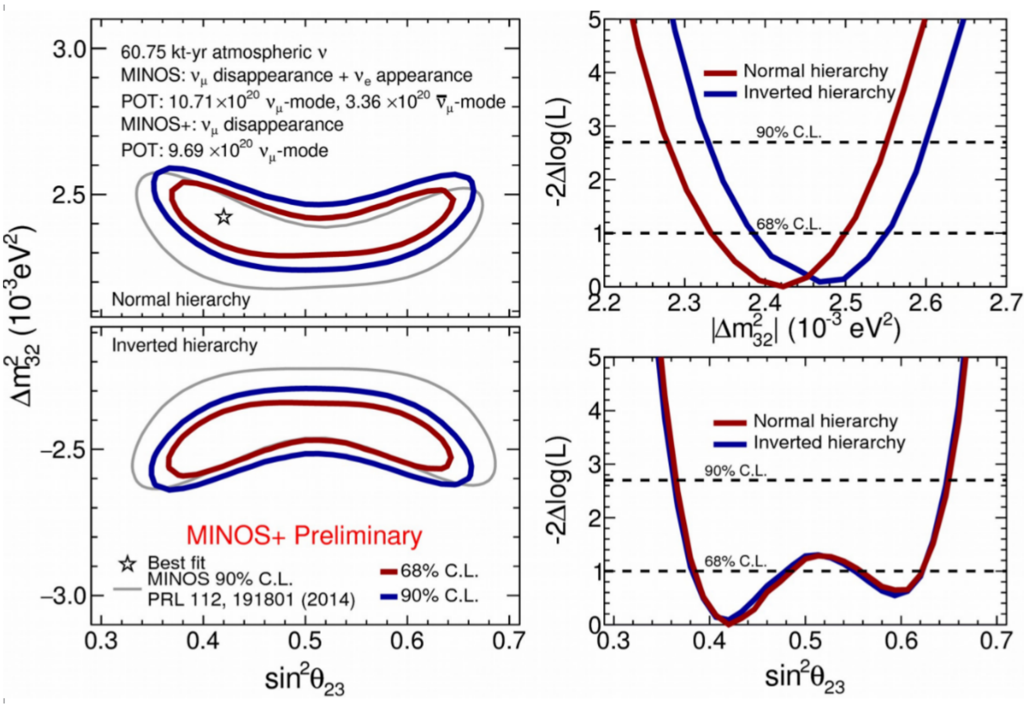

Figure 21: MINOS and MINOS+ latest combined results for θ_{23} and Δm^2_{32}. Left plot shows the 2D contours and best fit point for the Δm^2_{32} and the θ_{23} assuming both neutrino mass orderings. Rigth plots show the χ^2 curves for the Δm^2_{32} (top) and θ_{23} (bottom).

The value of Δm^2_{32} is consistent with the best fit values of the previous experiments and the results show a preference for the first octant of the θ_{23}, but values in the second octant are less than the 1σ away from the best fit point.
Finally, results also show a very slight preference for the normal neutrino mass ordering.

	Mass Ordering	$\sin^2\theta_{23}$	Δm^2_{32} (10^{-3} eV^2)
Best Fit	NH (slight pref.)	0.42	2.42

4 Results from Current LBL Neutrino Oscillation Experiments

Figure 22 summarizes the the results from all the reviewed experiments for the Δm^2_{32} and θ_{23} oscillation parameters.

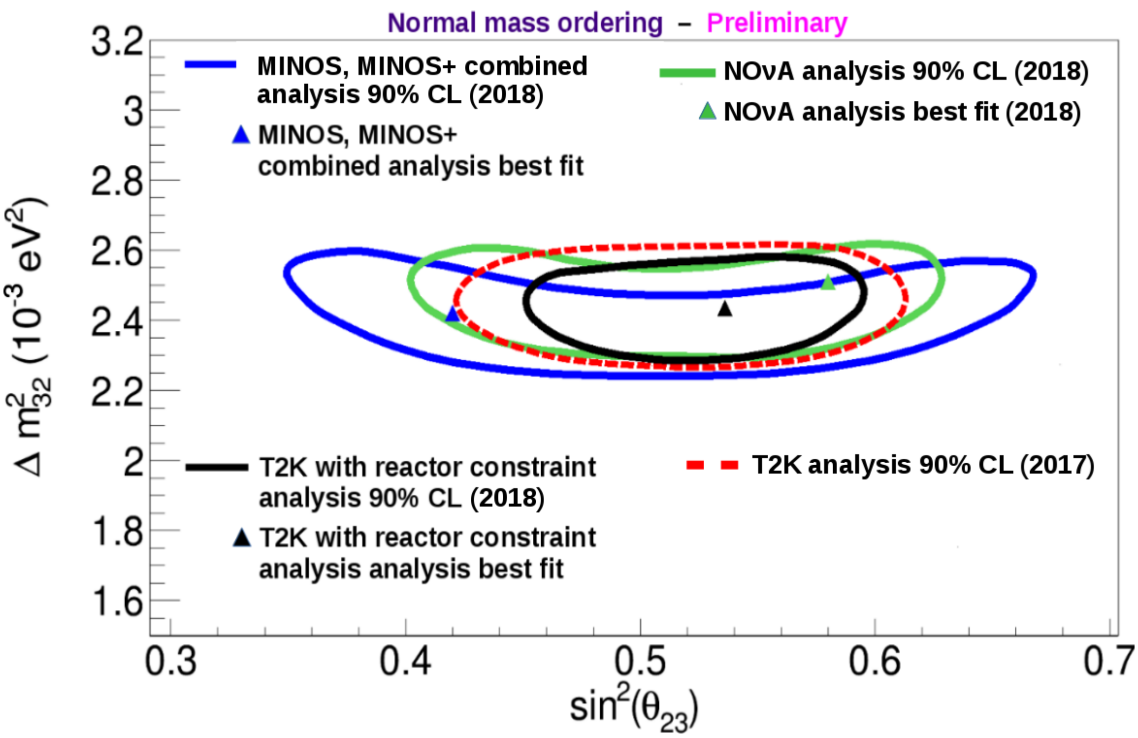

Figure 22: 90% confidence level 2D contours and best fit points for the Δm^2_{32} and θ_{23} for the T2K (dashed red), the T2K with reactor onstraints (black), the NOνA experiment and the MINOS and MINOS+ experiments.

All the described experiments show a preference for the normal ordering of neutrino masses for which the data is becoming more compelling. Something similar, but much less signifcant, happens for the CP phase, for which T2K and NOνA experiments prefer large and negative values of it and disfavouring CP-conserving values.
These results show the need for the T2K and NOνA joint analysis because it will provide a more clear picture of the remaining neutrino oscillation parameters.

5 Conclusion

The three main, currently operating, LBL neutrino experiments, T2K, NOνA and MINOS/MINOS+ have been reviewed and their most important results for the three neutrino oscillations shown.
In terms of neutrino oscillation results, all three experiments show a preference for normal neutrino mass ordering and NOνA and T2K data prefer the second octant of θ_{23} and, large negative values (close to $-\pi/2$) of δ_{CP}, disfavouring CP-conservation in the lepton sector. MINOS and MINOS+ best fit is at the first octant of θ_{23}, although compatible

with the second octant preference from the other experiments at $< 1\sigma$.
T2K will keep taking data until 2026 with improved neutrino beam and near and far detectors with the goal of $20 \cdot 10^{21}$ POT accumulated. In addition, a proposed joint fit of NOνA and T2K data will improve the sensitivity for the neutrino oscillation parameters, with special emphasis for the CP phase.
All these experiments are currently running and will continue to acquire data until the next generation experiments become operational, setting the basis to achieve precise measurements of all the neutrino oscillation parameters.

Acknowledgements

I would like to thank the organizers of the 15^{th} Tau Lepton Physics Workshop the T2K collaboration and the NOνA and MINOS experiemnts for giving me the opportunity to give this review talk dealing with the current status of the neutrino oscillation reaserch within long-baseline experiments.

Funding information This has been partially funded by the project *Física de oscilaciones de neutrinos en el IFIC y la UAM*, FPA2016-78417-C2-1-P, of the Spanish state agency, Ministerio de Economia y Competitividad.

References

[1] T2K Collaboration, *Search for CP violation in Neutrino and Antineutrino Oscillations by the T2K experiment with 2.2E21 protons on target*, Phys. Rev. Lett. 121 (2018) 17, 171802

[2] T2K Collaboration, *The T2K Experiment*, Physics Research A 659 (2011) 106–135

[3] T2K Collaboration, `http://t2k-experiment.org/2018/01/t2k-nova-announce`

[4] T2K Collaboration, *Measurement of the ν_μ CCQE cross section on carbon with the ND280 detector at T2K*, Phys. Rev. D 92, 112003 (2015)

[5] T2K Collaboration, *Measurement of muon-antineutrino and neutrino charged-current inclusive cross sections and their ratio with the T2K off-axis near detector*, Phys.Rev. D96 (2017)

[6] NOνA, *New constraints on oscillation parameters from ν_e appearance and ν_μ disappearance in the NOνA experiment*, Phys. Rev. D 98, 032012

[7] NOνA Collaboration, *Constraints on Oscillation Parameters from ν_e Appearance and ν_μ Disappearance in NOνA*, Phys. Rev. Lett. 118, 231801

[8] NOνA Collaboration, *Measurement of the Neutrino Mixing Angle θ_{23} in NOνA*, Phys. Rev. Lett. 118, 151802

[9] NOνA Collaboration, *First Measurement of Electron Neutrino Appearance in NOνA*, Phys. Rev. Lett. 116, 151806

[10] MINOS Collaboration, *The NuMI neutrino beam*, Nucl.Instrum.Meth. in Physics Research A. 806(2016)279-306

[11] MINOS Collaboration, *Combined analysis of muon-neutrino disappearance and muon-neutrino to electron-neutrino appearance in MINOS using accelerator and atmospheric neutrinos*, Phys.Rev.Lett.112.191801(2014)

[12] MINOS Collaboration, *Electron neutrino and antineutrino appearance in the full MINOS data sample*, Phys.Rev.Lett.110.171801(2013)

[13] MINOS Collaboration, *The Magnetized steel and scintillator calorimeters of the MINOS experiment*, Nucl. Instrum. Meth. A596 (2008) 190–228